

Design and Test of SiPM Readout Circuit

Kefan Li,^{a,*} Mingjie Yang,^{b,c,†} Shoushan Zhang,^{b,c} Long Chen^a and Fengrong Zhu^{a,†}

^a*Southwest Jiaotong University, School of Physical Science and Technology,
No. 999, Xi'an Road, Chengdu, China*

^b*Institute of High Energy Physics, Chinese Academy of Sciences, Key Laboratory of Particle
Astrophysics & Experimental Physics Division & Computing Center,
No. 19B Yuquan Road, Beijing, China*

^c*Institute of High Energy Physics, Chinese Academy of Sciences, TIANFU Cosmic Ray Research Center,
No. 1500 Kezhi Road, Chengdu, China*

E-mail: yangmingjie@ihep.ac.cn, zhufr@ihep.ac.cn

Silicon photomultiplier (SiPM) have several advantages such as high photon detection efficiency, wide spectral response range, high gain at low bias voltage and compact structure. In addition, SiPM is not damaged by high night sky background (NSB) level, which means that SiPM is a good choice for the atmospheric Cherenkov experiment such as LHAASO-WFCTA and The Cherenkov Telescope Array (CTA). However, the quenching resistor and capacitor inside SiPM will lead to a longer recovery when a photon causes avalanche inside SiPM, and then the pulse generated always has a much longer fall time than PMT. This work proposes a passive shaping circuit based on pole-zero cancellation circuit to realize the narrow pulse readout for SiPM without increasing power supply and the output pulse width has been reduced to under than 50 ns with the type of HAMAMATSU-S14466 and the size of 15 mm × 15 mm in the lab, when SiPM is illuminated by the 10 ns pulsed light.

38th International Cosmic Ray Conference (ICRC2023)
26 July - 3 August, 2023
Nagoya, Japan



*Speaker

1. Introduction

The Silicon Photomultiplier (SiPM) is a solid state photomultiplier comprised of a high density matrix of Geiger-mode-operated avalanche photodiodes also known as SPAD (single-photon avalanche photodiode) [1–3]. It offers several advantageous characteristics, including high gain at low bias voltage, high photon detection efficiency, immunity to magnetic fields, compact structure, and resistance to excess light. Figure 1 (a) illustrates the fundamental unit of SiPM, comprising a SPAD and a quenching resistor. A strong electric field exists inside the SPAD, and when a photon enters the SPAD and creates a pair of electron-hole pairs through the photoionization effect, the electrons in the electron-hole pairs are accelerated, collided, multiplied, and avalanched in that strong electric field. Without external intervention, the avalanche count would experience exponential growth until the component burns out. It is therefore necessary to add a large resistor RQ in series with the SPAD operating circuit to quench the avalanche.

The maximum avalanche current $I(f)$ generated by the SPAD avalanche quenching circuit (Figure 1 (a)) is calculated as follows:

$$I_f = \frac{V_{bias} - V_{br}}{RQ} \quad (1)$$

Where RQ is the resistance value of the quenching resistor, V_{bias} is the bias voltage between the cathode and anode of SPAD; V_{br} is the breakdown voltage of SPAD.

To the SiPM, a large number of SPAD microcells are connected electronically and arranged in two demensions. Figure 1 (b) shows a typical SiPM equivalent circuit, with a virtual junction capacitor attached to each SPAD and quenching resistor Rq [4]. The quenching resistor inside SiPM can protect it from the high and continuous illumination (like night sky background or the moonlight), which make SiPM can replace traditional Photomultiplier (PMT) in atmospheric Atmosphere Cherenkov experiment, such as LHAASO-WFCTA and CTA [5]. In addition, SiPM is frequently used in fields such as high-energy physics, medical imaging, and photon counting.

During application, the size of SiPM should match the design parameter of the detector. For example, the SiPM adopted by the LHAASO-WFCTA experiment has a size of 15 mm × 15 mm to match the optical design of the telescope increased and dynamic range of the camera. A larger area of SiPM means it has a larger dynamic range. However, due to the capacitance effect, the SiPM pulse width widens as the number of SPAD microcells increases [6]. To avoid energy leakage, a longer charge integration time window will be used for the long pulse width. Because the distribution of night sky background light in time is random, this introduces more night sky background light, and then the interference of NSB to effective signal pulse is increased.

In order to solve the problem, other teams have adopted a high bandwidth transconductance amplification circuit to achieve narrow pulse readout [7]. This method effectively shortens the pulse width, but increases the requirements for power and heat dissipation. In this article, we introduce a passive pole zero elimination circuit to process pulse. This passive circuit does not consume additional power, and can achieve the effect of narrowing the pulse width. The circuit design, debugging, and results will be detailed in the following chapters.

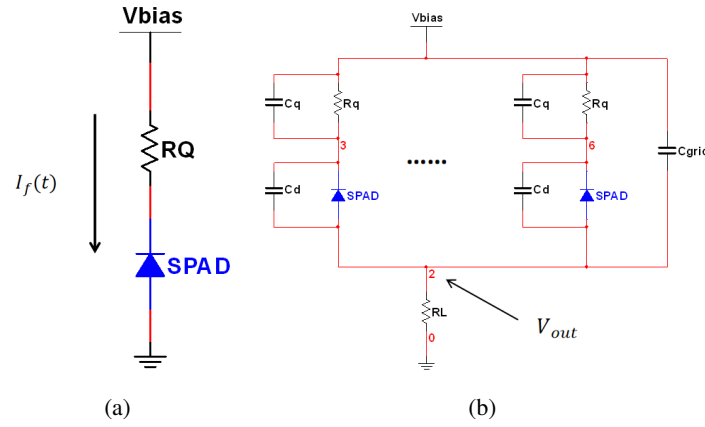


Figure 1: (a) Equivalent circuit model for a single SPAD, which is operating in Geiger mode. The quenching resistor RQ is used to protect SPAD from the thermal damage caused by avalanche. (b) SiPM Equivalent Circuit Model Composed of SPADs, an array of multiple SPADs inside the SiPM enables it to count a certain number of photons simultaneously[4].

2. Experimental design

2.1 The basic principle of pole zero cancellation circuit

To realize the narrow pulse readout, active shaping filter circuit and passive shaping filter circuit are commonly adopted[8]. These circuits can be used to obtain a pulse shape that meets the requirement by selecting the appropriate filter type and parameters. Active shaping filter circuits use active components, such as amplifiers, to shape signal pulse. On the other hand, passive shaping filter circuits do not use amplifiers or other active components, but rely on passive components such as capacitors and resistors. The pulse shape can be optimized by designing a suitable circuit network and configuring the matching circuit parameters.

Differential circuit is a common type of passive shaping filter to reduce the low frequency noise in the signal pulse and shorten the pulse fall time[9]. As shown in equation (2), when the input pulse of SiPM is in the form of exponential decay, it results in a downshoot in the differential circuit, which does not allow for the purpose of narrow pulse readout. The pole-zero canceling circuit is obtained by adding a resistor network to the differential circuit(as is shown in Figure 2), and by adjusting the parameters in the circuit to match the time constant of the circuit with that of the signal, the downshoot effect can be effectively eliminated. And at the same time the width of the signal is made narrower. The process of utilizing a pole-zero cancellation circuit to achieve a narrow pulse readout is described in detail in subsequent sections.

The pulse generated by SiPM obeys an exponential decay law with the time constant of τ . This law can be described by the following equation:

$$V_i(t) = \frac{Q}{C_d} e^{-\frac{t}{\tau}} \quad (2)$$

where C_d is the equivalent capacitance of the SiPM, Q is the total charge after avalanche inside SiPM, and τ is the time constant after the combination of SiPM's own circuit parameters and the

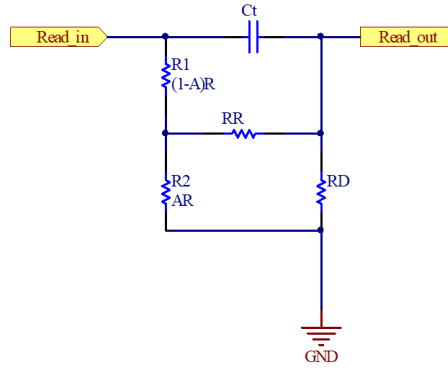


Figure 2: Schematic diagram of pole zero cancellation circuit

readout circuit.

The frequency domain signal of the pulse can be obtained from the Laplace transform by the above equation as follows:

$$V_i(S) = \frac{Q}{C_d} \times \frac{1}{S + \frac{1}{\tau}} \quad (3)$$

The transfer function (in Figure 2) of the pole zero cancellation circuit is as follows:

$$H(S) = \frac{S + \frac{1}{\tau_1}}{S + \frac{1}{\tau_2}} \quad (4)$$

The frequency domain expression of the output signal is shown below:

$$V_o(S) = V_i(S) \times H(s) = \frac{Q}{C_d} \times \frac{1}{S + \frac{1}{\tau}} \times \frac{S + \frac{1}{\tau_1}}{S + \frac{1}{\tau_2}} \quad (5)$$

where $\tau_1 = (C_t \times RR) / A$, $\tau_2 = (RR/RD) \times C_t$, $R_1 + R_2 = R$.

When $\tau_1 = \tau$ the output pulse becomes a unipolar pulse with a time constant of τ_2 :

$$V_o(S) = \frac{Q}{C_d} \times \frac{1}{S + \frac{1}{\tau_2}} \quad (6)$$

The obtained frequency domain expression is then subjected to inverse Laplace transform to obtain the time domain expression of the output pulse, as follows:

$$V_o(t) = \frac{Q}{C_d} e^{-\frac{t}{\tau_2}} \quad (7)$$

Consequently, after passing through the pole-zero canceling circuit, the unipolar pulse with a time constant of τ is changed to a unipolar pulse with a time constant of τ_2 . As the result, the pole-zero canceling circuit can realize narrow pulse readout for SiPM.

2.2 Test block diagram and device selection

Figure 3 (a) shows the block diagram of the whole experiment. 9 channels of SiPM with the type of S14466 from HAMAMATSU is adopted to test the performance of the PZC circuit. The test experiment is operated in a dark box, where the SiPM is illuminated by a pulse light. The pulse light is emitted by a LED with a wavelength of 405nm outside the dark box and transmitted into the dark box through a optical fiber. To obtain a uniform light distribution inside the dark box, an optical fiber beam expander with a diameter of 60mm is adopted to couple to the optical fiber.

Figure 3 (b) shows the circuit diagram of the experiment. The anodes of the 9 channel SiPMs are common connected, and the cathodes of them are common connected through a R-C circuit in serial. The R-C circuit is helpful to reduce the noise crosstalk among the 9 SiPMs.

Table 1: Main characteristics of the type of sensor used

Parameters	S14466	
Recommended operating voltage	60.5	(V)
Effective photosensitive area /channel	5(X)×5(Y)	(mm)
Number of pixels /channel	40,000	
Pixel size	25	(um)
Number of channel	9	ch
Gain	1.1×10^6	

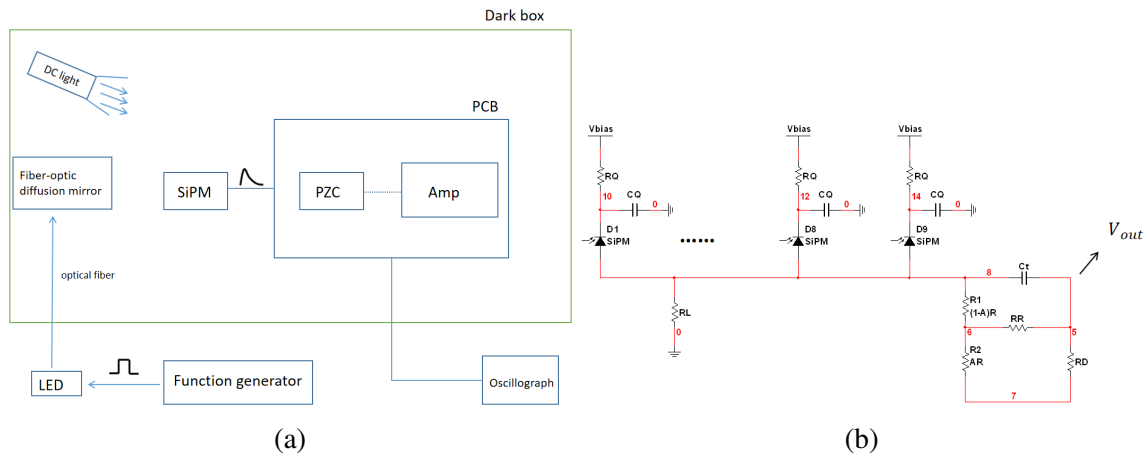


Figure 3: (a) is the block diagram of the experiment. The narrow pulse readout system is tested in a dark box. The LED light source is driven by a function generator, and width of the light pulse from the LED can be adjusted by the function generator. The signal of test system is transmitted to the oscillograph by coaxial cable. (b) shows the actual circuit diagram for the SiPM read-out, where 9 channels of SiPM with the size of 15 mm × 15 mm are spliced in parallel to form a large area SiPM with the size of 45 mm × 45 mm.

3. Test of the SiPM read-out circuit

Through matching the parameters of the circuit network (Fig 3(b)) to the time constant of the input pulse, we obtained a unipolar pulse with a width under 50 ns, as shown in Figure 4 (a).

In addition, we tested the response for the PZC circuit when SiPM is illuminated by both the pulse light and DC background light. The results are shown in Figure 4, which indicates that the pulse baseline is shifted upward and the pulse amplitude decreases, as the driving power of the LED light source increases. The increase of DC light will lead to the increase of the avalanching current for SiPM, and the protecting resistor RQ and the resistor RL serial with SiPM will obtain more voltage with the function of $V=I \times R$. As a result, the baseline from RL will rise with the DC light and the gain of SiPM will decrease. The results in Figure 4 show that when applied to atmospheric Cherenkov experiments, the narrow pulse readout method in this paper make NSB study is feasible.

Table 2: Model and parameters of the DC light source used

Electrical & Optical Characteristics	HSE405H-M807	
Power Dissipation	3000	(mW)
Peak Wavelength	405	(nm)
Viewing Half Angle	± 7	(deg)

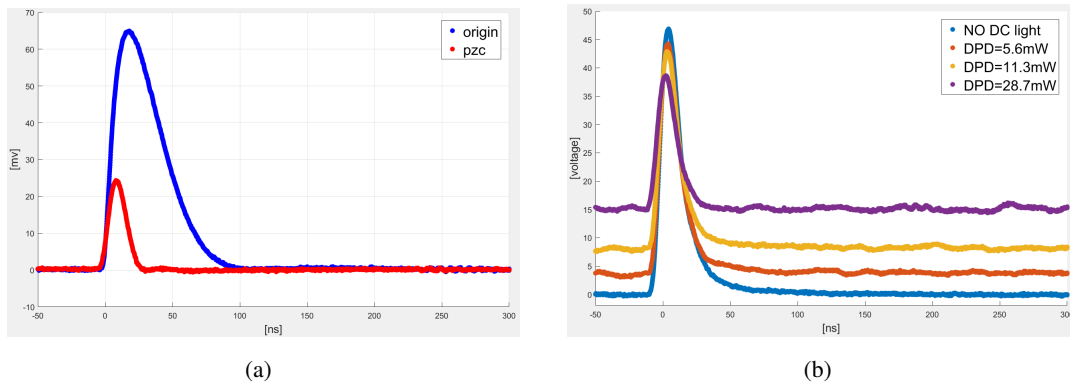


Figure 4: (a):The original pulse (blue) generated by SiPM illuminated by a 10 ns pulse light and the pulse passing through the PZC circuit (red). (b):Pulses readout from PZC circuit ,when SiPM is illuminated by both DC light and 10 ns pulse light. The SiPM readout circuit responds to different DC light, and a LED light source with a wavelength of 405 nm is fixed at a vertical distance of 30 cm from the SiPM. The DC light is emitted by a LED driven by a adjustable DC power.The DPD means the dirving power dissipation(DPD) for the LED light source.

In the Atmosphere Cherenkov experiment, the arrival duration time of the Cherenkov light is not a fixed value. In order to test the compatibility of the PZC circuit to the pulse light with different luminescence duration time, we let SiPM illuminated by the pulse light with different luminescence duration time varying from 14 ns-50 ns. The original pulse and the pulse after the PZC circuit are shown in Figure 5. There is no obvious overshoot found on the pulses, and the results indicate that the PZC circuit is compatible with pulse light durations from 14ns to 50ns.

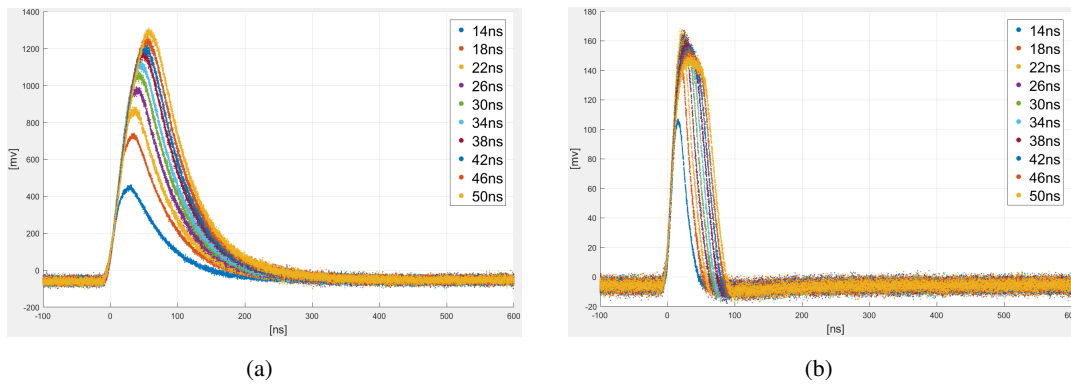


Figure 5: Pulses when SiPM is illuminated by pulse light with the luminescence duration time ranging from 14 ns to 50 ns, (a) represents the original pulse generated by SiPM, while (b) represents the pulse after the pole-zero canceling circuit.

4. Summary

In this work, we realize the narrow pulse readout for large area SiPM based on the pole-zero canceling (PZC) circuit. As the results presented in the paper, the PZC circuit is compatible with pulse light durations from 14 ns to 50 ns and allows for background light study for SiPM detector. The other performance, like linearity, signal-noise-ratio, charge resolution need to be evaluated in our next work. On the other hand, the PZC circuit not only narrow the pulse, but also make the pulse amplitude smaller. To resolve the problem, the low power amplifier will be added to the back-end electronics in the future, and the preliminary result is shown in Figure 6.

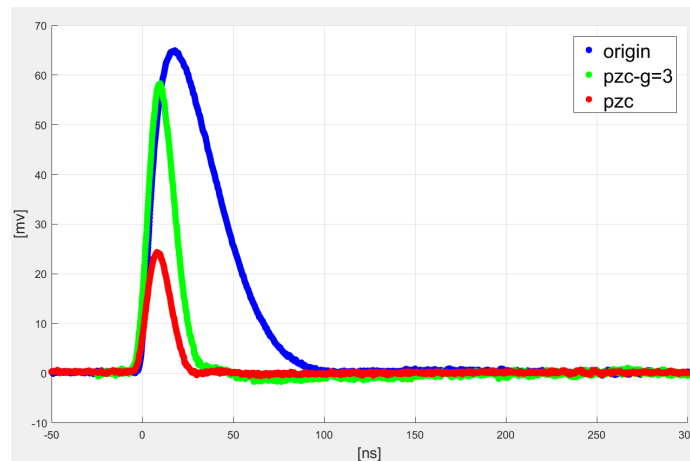


Figure 6: Blue: The origin pulse generated by SiPM. Red: The pulse after narrow pulse readout. Green: the pulse passes through a narrow pulse readout and then through an operational amplifier.

Acknowledgement

This work is supported by the National Natural Science Foundation of China (NSFC, No. 11905240).

References

- [1] D Renker. Geiger-mode avalanche photodiodes, history, properties and problems. *Nuclear Instruments & Methods in Physics Research. Section A, Accelerators, Spectrometers, Detectors and Associated Equipment*, 567(1):p. 48–56, 2006.
- [2] Thomas Frach, Gordian Prescher, Carsten Degenhardt, Rik De Gruyter, Anja Schmitz, and Rob Ballizany. The digital silicon photomultiplier—principle of operation and intrinsic detector performance. In *2009 IEEE Nuclear Science Symposium Conference Record (NSS/MIC)*, pages 1959–1965. IEEE, 2009.
- [3] Z., Liu, S., Gundacker, M., Pizzichemi, A., Ghezzi, E., and Auffray and. In-depth study of single photon time resolution for the philips digital silicon photomultiplier. *Journal of Instrumentation*, 11(06), 2016.
- [4] Fabio Acerbi and Stefan Gundacker. Understanding and simulating sipms. *Nuclear Instruments and Methods in Physics Research Section A: Accelerators, Spectrometers, Detectors and Associated Equipment*, 926:16–35, 2019.
- [5] BS Acharya, M Actis, T Aghajani, G Agnetta, J Aguilar, F Aharonian, Marco Ajello, A Akhperjanian, M Alcubierre, J Aleksić, et al. Introducing the cta concept. *Astroparticle physics*, 43:3–18, 2013.
- [6] F. Corsi, A. Dragone, C. Marzocca, A. Del Guerra, P. Delizia, N. Dinu, C. Piemonte, M. Boscardin, and G. F. Dalla Betta. Modelling a silicon photomultiplier (sipm) as a signal source for optimum front-end design. *Nuclear Instruments & Methods in Physics Research*, 572(1):416–418, 2007.
- [7] J. A. Aguilar, W. Bilnik, J. Borkowski, F. Cadoux, A. Christov, and Et Al. The front-end electronics and slow control of large area sipm for the sst-1m camera developed for the cta experiment. *Nuclear Instruments & Methods in Physics Research*, 830(sep.11):219–232, 2016.
- [8] Marco C. Campi. The problem of pole-zero cancellation in transfer function identification and application to adaptive stabilization. *Automatica*, 32(6):849–857, 1996.
- [9] Jitendra Tahalyani, M Jaleel Akhtar, Jayesh Cherusseri, and Kamal K Kar. Characteristics of capacitor: fundamental aspects. *Handbook of Nanocomposite Supercapacitor Materials I: Characteristics*, pages 1–51, 2020.